Electronic Supplementary Information for

Enhancing potassium-ion battery performance by defect and interlayer engineering

Yang Xu,[†*a] Farzaneh Bahmani,[†ab] Min Zhou,[a] Yueliang Li,[c] Chenglin Zhang,[a] Feng Liang,[d] Sayed Habib Kazemi,[b] Ute Kaiser,[c] Guowen Meng [*e] and Yong Lei [*a]

[a] Fachgebiet Angewandte Nanophysik, Institut für Physik & ZMN MacroNano (ZIK), Technische Universität Ilmenau, Ilmenau 98693, Germany

[b] Department of Chemistry, Institute for Advanced Studies in Basic Sciences, Zanjan 45137, Iran

[c] Central Facility for Electron Microscopy, Electron Microscopy Group of Materials Science, Ulm University, Ulm 89081, Germany

[d] State Key Laboratory of Complex Nonferrous Metal Resources Clean Utilization, Kunming University of Science and Technology, Kunming 650093, China

[e] Institute of Solid State Physics, Chinese Academy of Sciences, Hefei, Anhui 230031, China

[†] These authors contributed equally.

Corresponding authors:

Dr. Yang Xu: yang.xu@tu-ilmenau.de

Prof. Guowen Meng: gwmeng@issp.ac.cn

Prof. Yong Lei: yong.lei@tu-ilmenau.de

Experimental details

Materials synthesis: MoS_2 nanoflowers were synthesized using a hydrothermal method. In a typical procedure, 1 mmol $(NH_4)_6Mo_7O_{24}\cdot 4H_2O$ was dissolved in 35 ml DI water under stirring, and different amounts of thiourea were added to the solution. The obtained solution was kept stirring for 0.5 h and then transferred to a Teflon-lined stainless-steel autoclave. The autoclave was sealed and maintained at 210°C for 24 h. After cooling to room temperature naturally, the product was collected by centrifuging the mixture, rinsed with absolute ethanol several times, and then dried in vacuum at 60°C. Interlayer-expended and defect-rich MoS_2 was synthesized using 60 mmol thiourea, and defect-free MoS_2 was synthesized using 14 mmol thiourea.

Characterizations: Characterizations of the samples were carried out by X-ray diffractometry (D/MAX2500V PC diffractometer, Cu Kα $\lambda = 1.54$ Å), Raman spectroscopy (inVia Raman microscope), X-ray photoelectron spectroscopy (Thermo SCIENTIFIC ESCALAB 250Xi), scanning electron microscopy (Hitachi S4800), FEI Titan 80-300 aberration-corrected transmission electron microscopy (80 kV).

Electrochemical measurements: The electrodes were fabricated by mixing the active material, Super P and poly(vinylidenedifluoride) (PVDF) at a weight ratio of 70:20:10, then coated uniformly (doctor-blade) on a copper foil with a mass loading of ~1.0 mg cm^{-2}. The electrodes were dried at 110°C under vacuum for more than 12 h. Electrochemical tests were carried out using coin cells, CR2032, which were assembled in a nitrogen-filled glovebox with oxygen and moisture concentrations kept below 0.1 ppm. K foil used as counter electrode was separated from working electrode by a glass microfiber filter (Whatman, Grade GF/B). The electrolyte was 1 M potassium bis(fluorosulfonyl)imide (KFSI) in an ethylene carbonate (EC)/diethylene carbonate (DEC) solution (1:1). Cyclic voltammetry and electrochemical galvanostatic intermittent titration were performed on a VSP electrochemical workstation (Bio-Logic, France). Electrodes were discharged at a series of current density of 20 mA g^{-1} pulses for 15 min and left on open circuit for 2 h relaxation after each pulse to reach an equilibrium potential. Galvanostatic charge/discharge was performed on a Land CT 2001A battery testing system (Land, China) at room temperature.

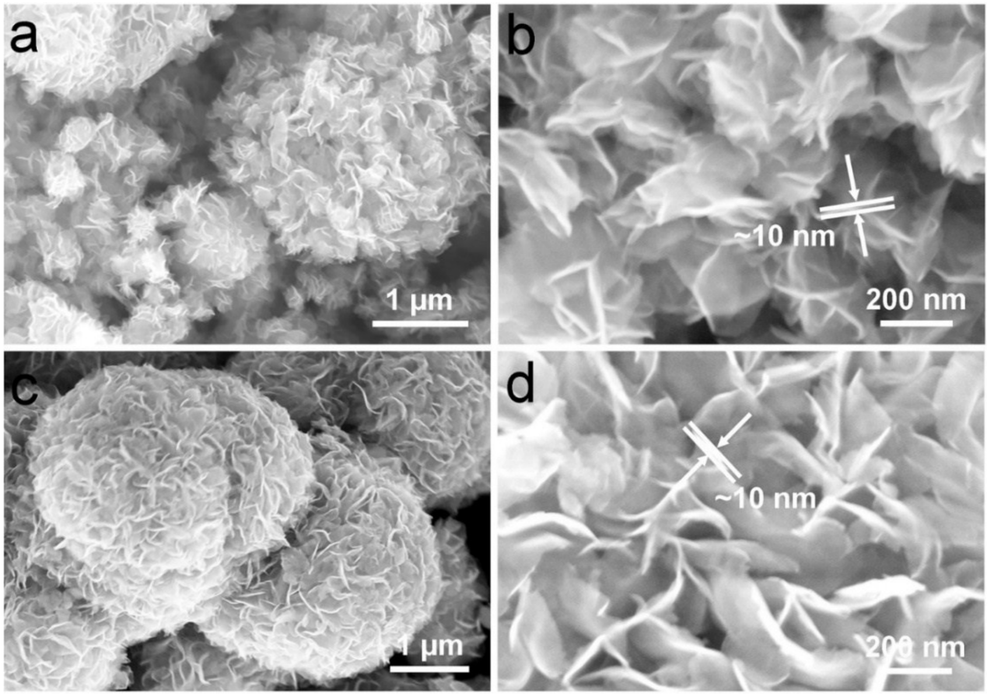

Fig. S1. SEM images of D-MoS_2 NFs (a and b) and MoS_2 NFs (c and d).

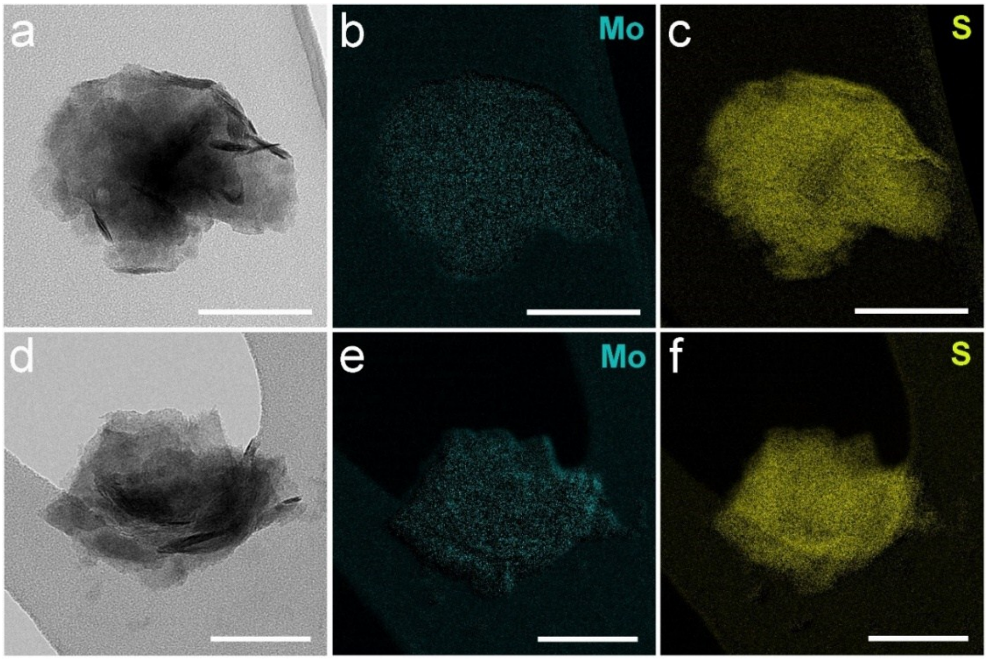

Fig. S2. TEM bright-field images of D-MoS_2 NFs (a) and MoS_2 NFs (d). Three-window elemental maps of D-MoS_2 NFs (b: Mo; c: S) and MoS_2 NFs (e: Mo; f: S). Scale bars: 100 nm.

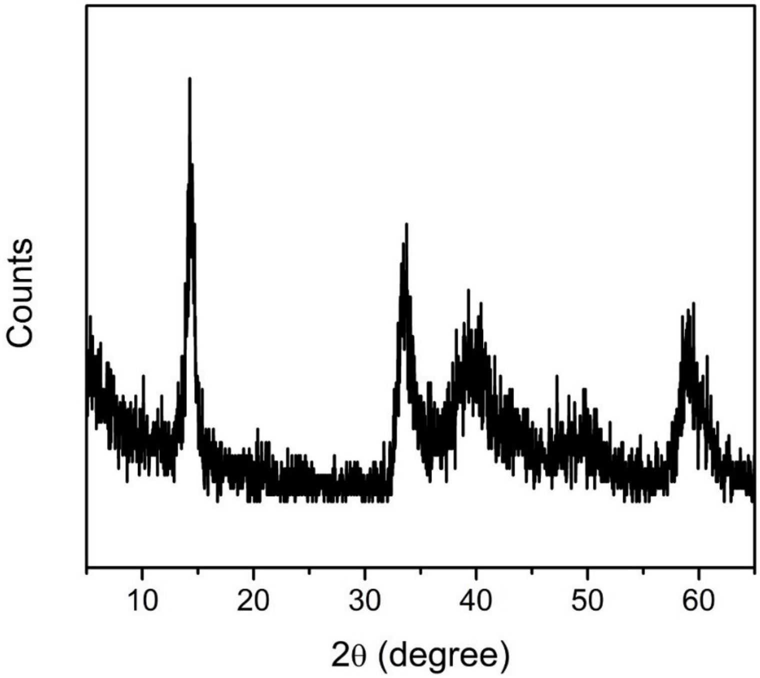

Fig. S3. XRD pattern of D-MoS_2 NFs after annealing at 700°C for 3 h.

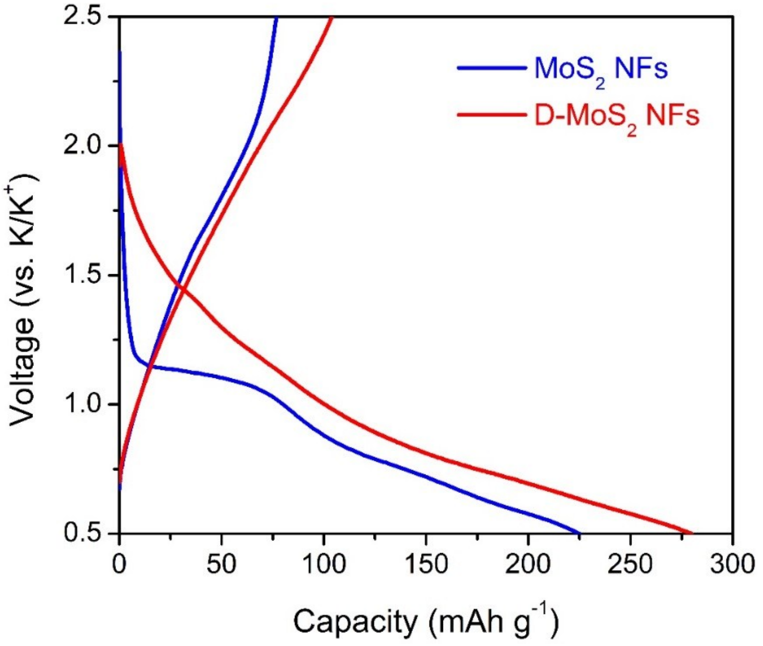

Fig. S4. Discharge-charge profiles of D-MoS$_2$ and MoS$_2$ NFs at cycle1.

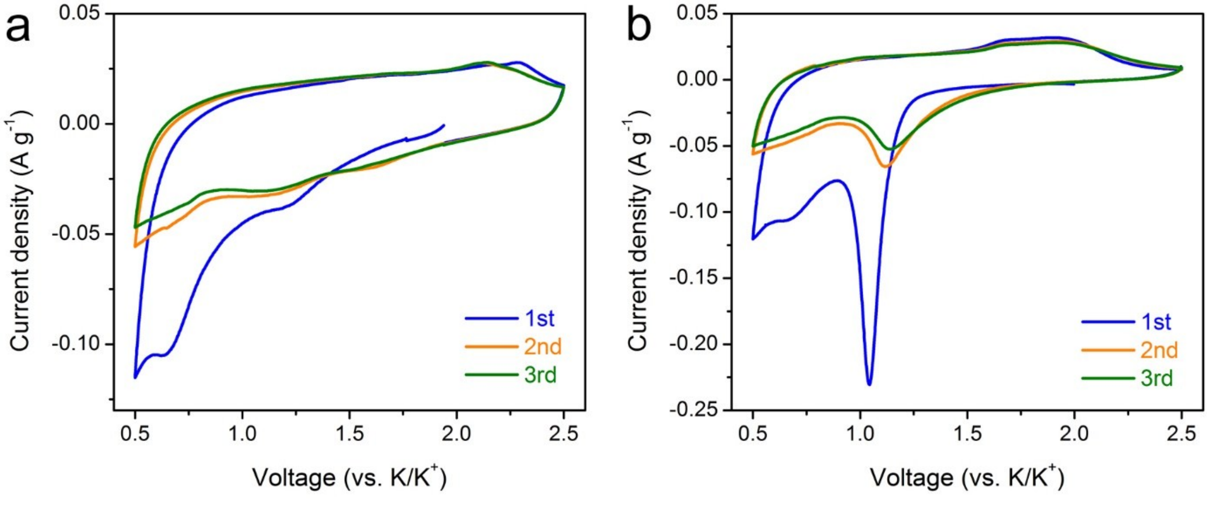

Fig. S5. CV curves of D-MoS$_2$ NFs (a) and MoS$_2$ NFs (b).

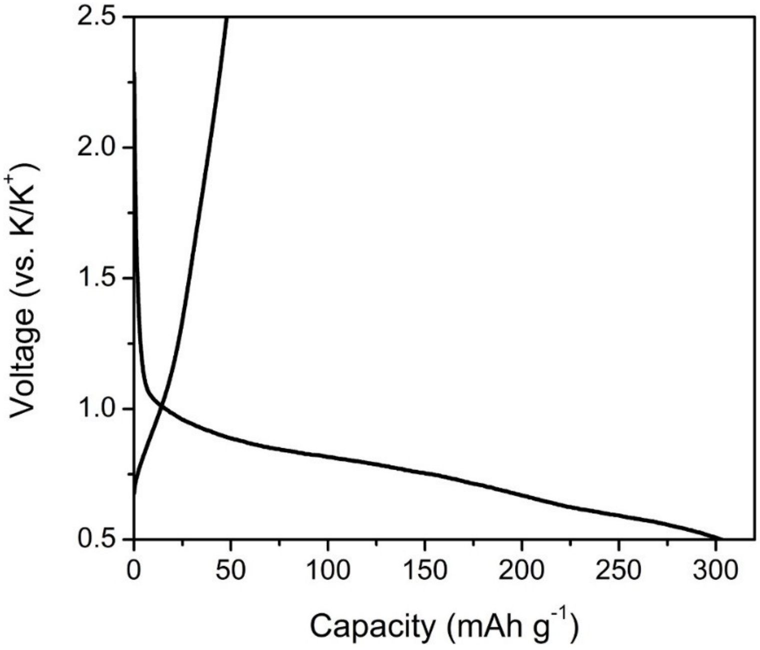

Fig. S6. Discharge-charge profiles of Super P at cycle1. The electrode was prepared by mixing Super P and PVDF using a weight ratio of 2:1. The discharge and charge capacities are 303 and 48 mAh g^{-1}, giving a CE of 16%.

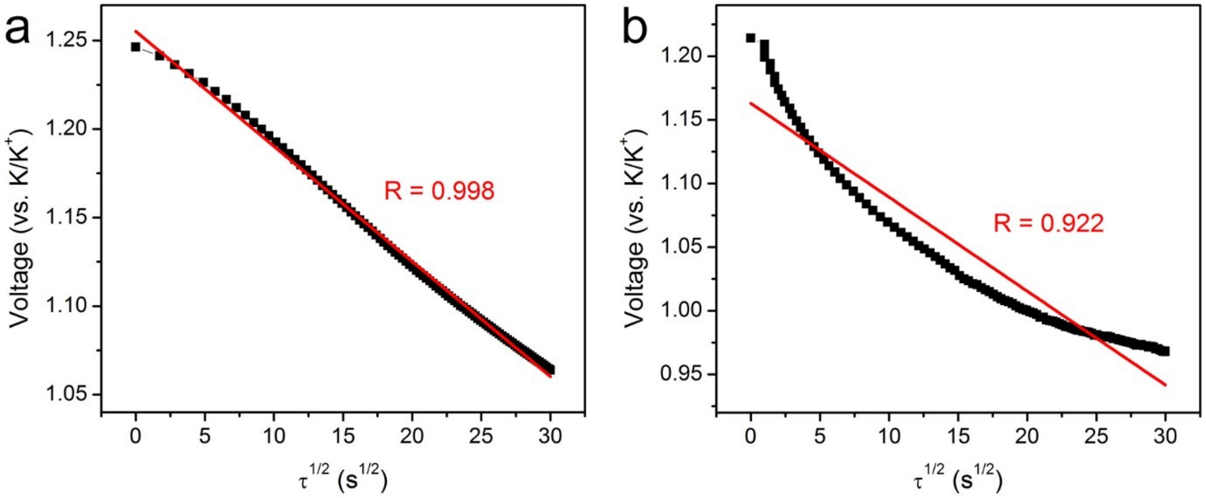

Fig. S7. The relationship between the voltage change and the square root of relaxation time for D-MoS$_2$ NFs at 1.33 V (a) and MoS$_2$ NFs at 1.51 V (b). The relationship is linear or quasi-linear, which is the prerequisite for the calculation of D_k, as described in the next figure.

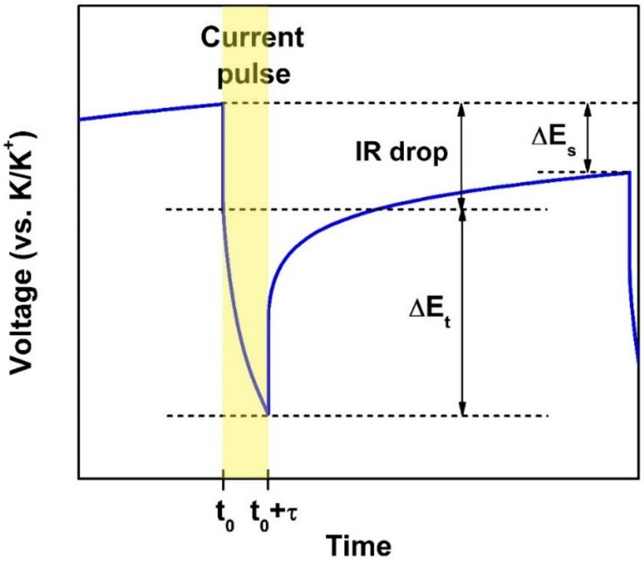

Fig. S8. Schematic of the calculation of diffusion coefficient using the GITT technique.

The diffusion coefficient is calculated according to the following equation if the cell potential is linearly proportional to $\tau^{1/2}$:[1,2]

$$D = \frac{4}{\pi\tau}\left(\frac{m_b V_M}{M_B S}\right)^2\left(\frac{\Delta E_s}{\Delta E_t}\right)^2 \quad \left(t \ll \frac{L^2}{D}\right)$$

where τ is the current pulse time (s), m_b is the mass of the active material, M_B is the molar mass of the active material, V_M is the molar volume of the active material, S is the geometric area of the electrode, and ΔE_s and ΔE_t are defined as shown in the figure.

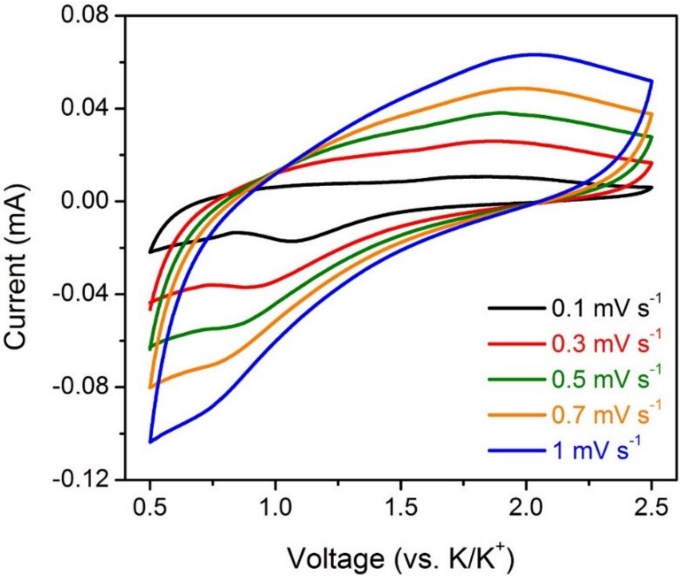

Fig. S9. CV curves of MoS_2 NFs at various scan rates.

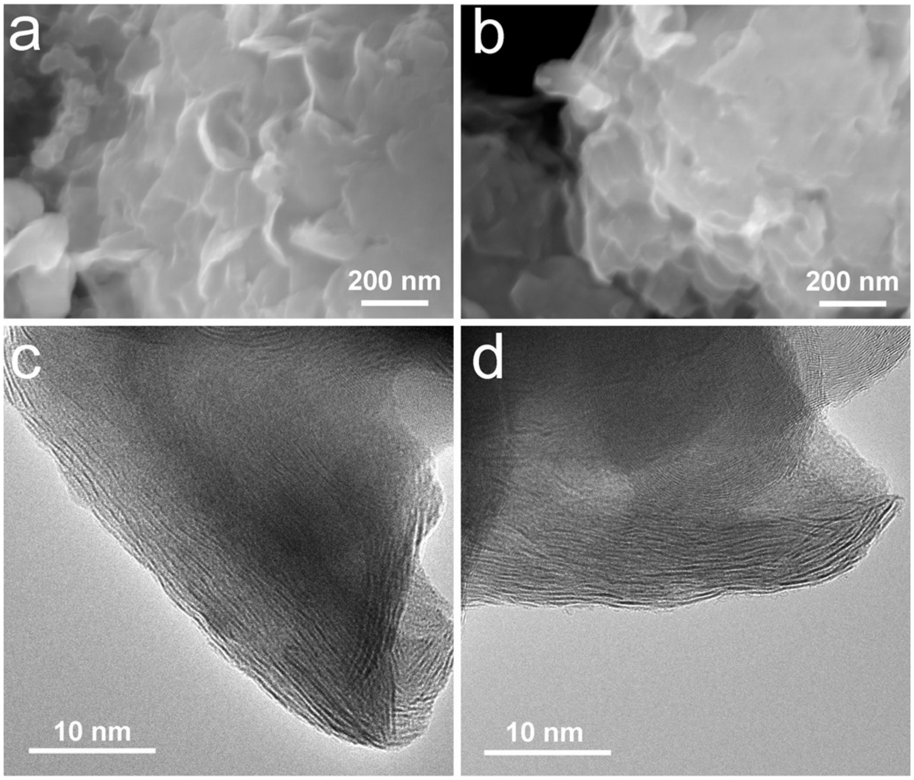

Fig. S10. SEM (a and b) and TEM (c and d) of D-MoS_2 NFs (a and c) and MoS_2 NFs (b and d) after 100 cycles.

References

[1] W. Weppner and R. A. Huggins, *J. Solid State Chem.*, 1977, **22**, 297-308.

[2] Z. Jian, Z. Xing, C. Bommier, Z. Li and X. Ji, *Adv. Energy Mater.*, 2016, **6**, 1501874.